METRIC ACCURAC TESTING WITH MOBILE PHONE CAMERAS

Armin Gruen, Devrim Akca *

Institute of Geodesy and Photogrammetry, ETH Zurich, CH-8093 Zurich, Switzerland - (agruen, akca)@geod.baug.ethz.ch

Commission V, WG-V-5

KEY WORDS: Mobile phone cameras, Self-calibration, Accuracy potential, JPEG test, Stability test.

ABSTRACT:

This paper examines the potential of mobile phones to be used as a front-end sensor for photogrammetric procedures and applications. For this purpose we are calibrating two mobile phones (Sony Ericsson K750i and Nokia N93) over our indoor 3D testfield, using self-calibration. Using the same testfield we are performing accuracy tests in order to evaluate the metric performance and comparing them with respect to two off-the-shelf digital still video cameras (Sony DSC W100 and Sony DSC F828). In some systems we have diagnosed substantial systematic errors. We find that the JPEG compression does not significantly influence the errors. We are currently also in the process of checking the stability of the interior orientation over time. This paper reports about our experiences in calibration and accuracy validation of mobile phone cameras. We believe that with a proper performance these devices can be used for many photogrammetric tasks in the future.

1. INTRODUCTION

Mobile Mapping has been an issue for ISPRS already for some years. Through the use of moving platforms (satellites, aerial, terrestrial) photogrammetry had from early times on a "mobile" component. Also, on-line and real-time processing is by no means new. However, with the availability of very affordable and good resolution CCD/CMOS cameras and other off-the-shelf devices, including compact computers (of laptop type) the potential of building efficient mobile systems has dramatically increased. On other occasions we have already reported on the use of an autonomous model helicopter for 3D modeling in different projects. Location-based services and ubiquitous computing are current busswords of high societal visibility and relevance. Among various hardware and software components mobile phones constitute an interesting component for image data acquisition for obvious reasons: They are very inexpensive, light and handy and have CMOS cameras of currently up to 10 Mpixels image format. This paper examines the potential of mobile phones to be used as a front-end sensor for photogrammetric procedures and applications.

Laptops do have nowadays so much processing power and storage capabilities that part of the model generation can be done in the field already. With available know-how and software modules in sequential estimation, semi-automated and automated triangulation and surface model generation and texturing, a good basis exists to build a system for mobile, field-based primary data acquisition and model building. We anticipate the (future) possibilities of on-line processing the acquired image data by mobile phone cameras. This opens the path for a paradigm shift from "Mobile Mapping" to "Mobile 3D Modeling".

Usability of mobile phone cameras for many applications has recently been realized. One of the most prominent applications is the character/text recognition in a flexible and portable

fashion (Watanabe et al., 2003; Koga et al., 2005; Parikh, 2005). Rohs (2004) realizes a scenario where camera phones are used to recognize the visual codes in the scene. By recognizing a code tag, the device determines the code value, the targeted object or image element. The phone's wireless communication channel is used to retrieve online content related to the selected image area or to trigger actions based on the sensed code.
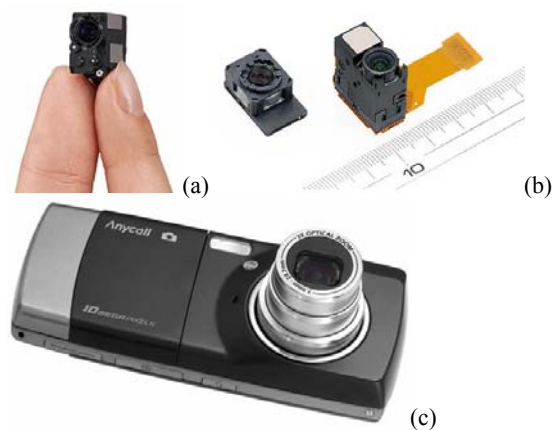

Figure 1. (a) Sharp's 2 Mpixel CCD camera module LZP0P3738, (b) Sharp's 3 Mpixel CCD camera modules LZ0P3751 and LZ0P3758, (c) Samsung's 10 Mpixel camera integrated handy SCH-B600.

As a facial animation study for mobile phones, Riegel (2005) creates a specific 2D head model using the generic 3D MPEG-4 face and portrait images. The model is animated via voice or text. Al-Baker et al. (2005) uses a GPRS and WAP enabled PDA or mobile phone for human face identification. The system allows the user to send an image of a human face, acquired through a mobile phone with a built-in camera, to

---

* Corresponding author. www.photogrammetry.ethz.ch

remotely perform automatic face recognition. The user will then instantly receive details of the person, if a match is found. The system can be useful especially for the instant face identification and authentication tasks. Clemens et al. (2005) develop a panoramic image application suit for handy cameras. The image stitching is carried out in real-time. Pittore et al. (2005) implement an image-based context awareness engine specifically for archeological sites and museums. Visitors can "ask" information about an unknown monument by simply taking a picture of it with a camera integrated mobile phone and send it to the system for recognition. Ueda et al. (2004) use mobile phones, equipped with a camera and a GPS chip, as a content provider to a Geographical Information System (GIS). Users can annotate objects in the environment by sending text, picture and location information via mobile phone to a central data base. Chung et al. (2004) correct the radial lens distortion of a mobile phone camera applying a calibration procedure from Lenz and Tsai (1988). However, their experiment lacks numerical results and analysis. In spite of the availability of a broad diversity of applications, the metric capabilities and characteristics of mobile phone cameras have not been investigated so far.

In 2004, Sharp Corporation developed a 2 Mpixel CCD camera module with 2X optical zoom and auto-focus function (Figure 1a) intended for use in mobile phones (Physorg, 2004). In 2005, they released two new camera modules (Figure 1b) with a 3 Mpixel CCD chip (Physorg, 2005). One year after, Samsung announced a 10 Mpixel camera phone (Figure 1c) at CeBIT exhibition in Hannover (Williams, 2006). These examples show the rapid progress in the technology of mobile phone cameras. Due to very limited size and restricted material and equipment costs, the production of mobile phone cameras is a challenge (Myung-Jin, 2005; Chowdhury et al., 2005). The impact of their production specifications on the stability of interior orientation and 3D object reconstruction capabilities has not adequately been studied yet. This work investigates the accuracy potential of two recent mobile phone cameras (Sony Ericsson K750i and Nokia N93) and compares them with respect to two off-the-

shelf digital still video cameras (Sony DSC W100 and Sony DSC F828). The next chapter introduces the cameras and the calibration/validation testfield. We carry out self-calibration, accuracy testing, JPEG testing and stability testing of the interior orientation over time, and report the results in the third chapter. We present a comparative analysis of the results in the fourth chapter.

2. CAMERAS AND THE TESTFIELD

2.1 Cameras

Four cameras are used (Figure 2). Two of them are mobile phone cameras (Sony Ericsson K750i and Nokia N93) and two of them are off-the-shelf digital still video cameras (Sony DSC W100 and Sony DSC F828). The mobile phone cameras have CMOS sensors of smaller size than the CCD chips in the off-the-shelf cameras and partly much smaller lenses. The technical specifications of all four cameras are given in Table 1.

2.2 Testfield

The photogrammetric calibration field at the Institute of Geodesy and Photogrammetry (HIL C57.3, ETH Zurich) was used. It is 3.4 x 2.0 x 1.0 m^3 in size. The 3D coordinates of 87 well distributed control points (GCP) were measured using a Leica Axyz system. The Leica Axyz system consists of two Leica total stations (TC 3000 and TC 2002) and one processing computer unit, which is connected to them (Figure 3). After an initialization step, two operators simultaneously measure the vertical angles and horizontal directions of the targeted point. The system calculates the 3D coordinates (by spatial intersection) and the precision values in real-time. The scale of the object space was given by measuring a bar whose length was accurately defined by interferometry as 1000.051 ±0.010 mm. The average theoretical precision values of the GCPs are ±0.03, ±0.05 and ±0.03 mm for X, Y and Z axes, respectively.

Figure 2. Cameras used in our tests: (a) Sony Ericsson K750i, (b) Nokia N93, (c) Sony DSC W100, (d) Sony DSC F828.

	K750i	N93	W100	F828
Sensor	CMOS	CMOS	CCD	CCD
	1/3.2" = 4.5 x 3.4 mm	1/3.2" = 4.5 x 3.4 mm	1/1.8" = 7.2 x 5.3 mm	2/3" = 8.8 x 6.6 mm
Pixel size	2.8 micron	2.2 micron	2.2 micron	2.7 micron
Image format	1632 x 1224	2048 x 1536	3264 x 2448	3264 x 2448
	2 Mpixel	3.2 Mpixel	8 Mpixel	8 Mpixel
Lens	No information	Carl Zeiss	Carl Zeiss	Carl Zeiss T*
		Vario-Tessar	Vario-Tessar	Vario-Sonnar
Focal length	4.8 mm	4.5 – 12.4 mm	7.9 – 23.7 mm	7.1 – 51.0 mm
Optical zoom	No	3X	3X	7X
Auto focus	Yes	Yes	Yes	Yes
Aperture	F/2.8 (fixed)	F/3.3 (fixed)	F/2.8 – F/5.2	F/2.0 – F/8.0
Output format	Only JPEG	Only JPEG	Only JPEG	JPEG and TIFF

Table 1. Technical specifications of the cameras.

3. ACCURACY TEST

For the calibration of the K750i, eighteen images from three locations (each of which has three stations, i.e., down, middle and up) were taken in a convergent geometry mode (Figure 4a). Nine images were taken in normal mode (image no. 1-9) and each three of the rest nine images are -90^0 (image no. 10-12), $+90^0$ (image no. 13-15) and 180^0 (image no. 16-18) rotated, respectively.
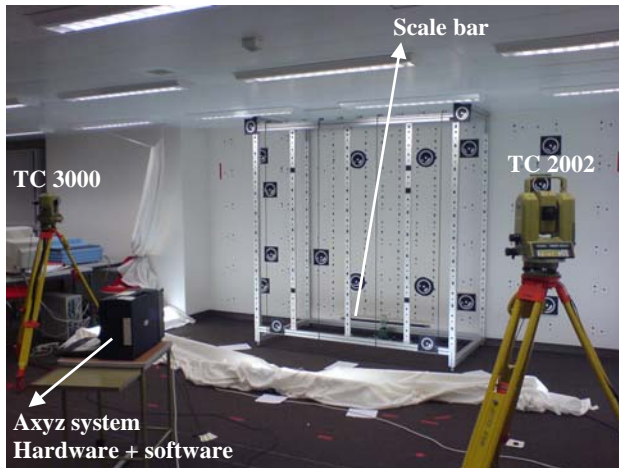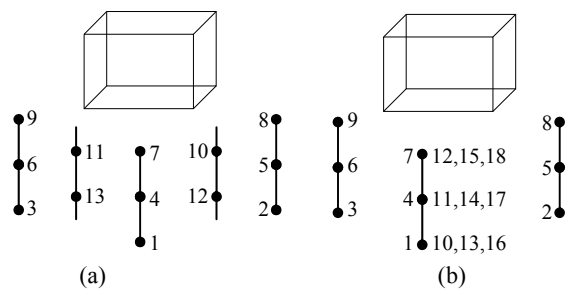

Figure 3. The 3D testfield and the Axyz system.

Figure 4. (a) Image acquisition geometry for the calibration of K750i, and (b) for N93, W100 and F828. Black circles stand for the image stations.

For the calibration of the N93, W100 and F828 cameras an image acquisition geometry with thirteen images (Figure 4b) was used. Images no. 1-9 are in normal mode and no. 10-13 are the rotated ones. However, different rotated image versions were used. For the camera N93 the images no. 10 and 11 were -90^0 and no. 12 and 13 were $+90^0$ rotated, for W100 no. 10-13 were all $+90^0$ rotated, and for F828 no. 11 and 13 were -90^0 and no. 10 and 12 were $+90^0$ rotated. For N93, W100 and F828 the focal length was set to the smallest possible value by zooming.
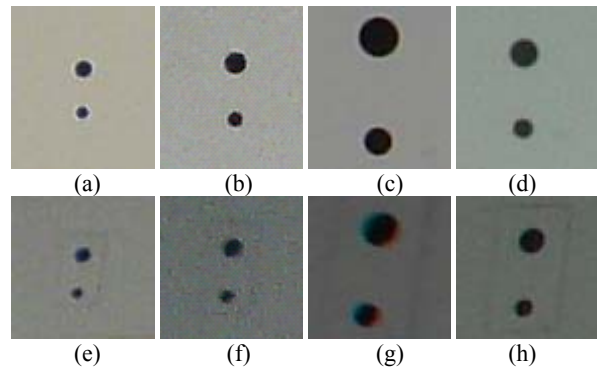

Figure 5. Image quality of the cameras. (a), (b), (c) and (d) are cropped images at station 4 from K750i, N93, W100 and F828, respectively. The signalized point approximately locates at the centre of the image. Image scales are 1/863, 1/829, 1/460 and 1/513 for (a), (b), (c) and (d), respectively. (e), (f), (g) and (h) are cropped images at station 1 from K750i, N93, W100 and F828, respectively. The signalized point approximately locates at the upper left part of the full image. Image scales are 1/977, 1/961, 1/550 and 1/583 for (e), (f), (g) and (h), respectively.

The image measurements were performed with the Least Squares template matching (Gruen, 1985) using the in-house developed software BAAP. Another in-house developed software SGAP (Beyer, 1992) was used for the bundle block adjustment with self-calibration.

The imaging quality differs among the cameras. In Figure 5a, 5b and 5c, low-level image enhancement effects are strongly visible at the edges of the points. The F828 has the best overall image quality considering all images from all stations. On N93 images (Figure 5b and 5f) strong JPEG artifacts are visible (Figure 6). The K750i, N93 and W100 have only the JPEG output option. Their image measurements were carried out on their original JPEG images. For the F828, TIFF output images were used for the image measurements.

Figure 6. 3X zoom-in of the upper left part of Figure 5f. JPEG artifacts are visible.

3.1 Accuracy test of K750i

The 18 images version gives a sigma0 value of about half a pixel (version 10 in Table 2) and highly systematic residual patterns in some images (Figure 7a and 7b), even after self-calibrating bundle adjustment with block-invariant additional parameters.

The six most deteriorated images among the rotated ones were then excluded (images no. 11, 12, 13, 14, 16 and 18). These reduced twelve images versions (versions 11, 12, 13, 14 and 15 in Table 2) give better sigma0 and precision values. However, a systematic pattern of the image coordinate residuals still remains, varying from image to image. Note that version 15 stands for the free network adjustment. After Brown's 10 additional parameter set, Gruen's (1978) 44 additional parameter set was applied. The block-invariant 44 additional parameters did not compensate the systematic errors as well (version 12).

3.2 Accuracy test of N93

The accuracy test of N93, also based on block-invariant APs, apparently gives better results. The sigma0 is a quarter of a pixel. A systematic error pattern still remains in the residuals (Figure 7c and 7d), however, the magnitude is much less than in the K750i's case. It has clearly achieved sub-millimeter

accuracy in object space (versions 22 and 23 in Table 3) in all coordinate directions.

3.3 Accuracy test of W100

The W100 gives slightly better theoretical precision and empirical accuracy values than the N93 (Table 4). The standard deviation of image observations is in the same range with the N93, i.e. one quarter of a pixel. The W100 reveals similar residual errors like the N93 regarding the magnitude (Figure 7e and 7f).

3.4 Accuracy test of F828

The F828 gives the best performance and remarkably superior numbers compared to the other cameras (Table 5). Sigma0 goes down to 1/10 of a pixel, satisfying the theoretical expectations of the Least Squares template matching. Also, the empirical RMSEs are here in much better agreement with the theoretical standard deviations.

Ver	GCP	CHK	TIE	APs	Rej	Sigma0	STD-X	STD-Y	STD-Z	RMSE-X	RMSE-Y	RMSE-Z
						μm/pixel	of CHK+TIE points (mm)			at CHK points (mm)		
10	87	0	90	10	0	**1.20/0.43**	**0.291**	**0.558**	**0.251**	N.A.	N.A.	N.A.
11	87	0	80	10	26[1]	**0.65/0.23**	**0.187**	**0.307**	**0.161**	N.A.	N.A.	N.A.
12	87	0	80	44	26[1]	**0.64/0.23**	**0.185**	**0.304**	**0.159**	N.A.	N.A.	N.A.
13	44	43	80	10	25[1]	**0.64/0.23**	**0.188**	**0.312**	**0.163**	0.280	0.498	0.201
14	10	77	80	10	27[1]	**0.61/0.22**	**0.196**	**0.318**	**0.173**	0.499	1.048	0.501
15	167	--	free	10	30[1]	**0.59/0.21**	**0.174**	**0.283**	**0.151**	N.A.	N.A.	N.A.

Table 2. Absolute accuracy test of K750i.

Ver	: Version number
GCP/CHK/TIE	: Number of control points / independent check points / tie points, respectively
APs	: Number of additional parameters
Rej	: Rejected rays by data–snooping, rejection rule for [1] : reject all residuals >= 4xSigma0
Sigma0	: Standard deviation of image observations a posteriori
STD	: Average theoretical precision values of CHK/TIE/GCP coordinates
RMSE	: Empirical accuracies of CHK/GCP coordinates.

Ver	GCP	CHK	TIE	APs	Rej	Sigma0	STD-X	STD-Y	STD-Z	RMSE-X	RMSE-Y	RMSE-Z
						μm/pixel	of CHK+TIE points (mm)			at CHK points (mm)		
21	87	0	99	10	0	**0.55/0.25**	**0.165**	**0.312**	**0.139**	N.A.	N.A.	N.A.
22	44	43	99	10	0	**0.52/0.24**	**0.157**	**0.286**	**0.133**	0.449	0.617	0.225
23	10	77	99	10	0	**0.50/0.23**	**0.161**	**0.284**	**0.140**	0.701	0.816	0.203
24	186	--	free	10	0	**0.47/0.21**	**0.144**	**0.250**	**0.120**	N.A.	N.A.	N.A.

Table 3. Absolute accuracy test of N93 (image acquisition on 6th February, 2007).

Ver	GCP	CHK	TIE	APs	Rej	Sigma0	STD-X	STD-Y	STD-Z	RMSE-X	RMSE-Y	RMSE-Z
						μm/pixel	of CHK+TIE points (mm)			at CHK points (mm)		
31	87	0	92	10	0	**0.59/0.27**	**0.114**	**0.203**	**0.094**	N.A.	N.A.	N.A.
32	44	43	92	10	0	**0.55/0.25**	**0.104**	**0.181**	**0.084**	0.298	0.369	0.221
33	10	77	92	10	0	**0.47/0.21**	**0.100**	**0.168**	**0.085**	0.501	0.421	0.443
34	179	--	free	10	0	**0.44/0.20**	**0.083**	**0.140**	**0.067**	N.A.	N.A.	N.A.

Table 4. Absolute accuracy test of W100.

Ver	GCP	CHK	TIE	APs	Rej	Sigma0	STD-X	STD-Y	STD-Z	RMSE-X	RMSE-Y	RMSE-Z
						μm/pixel	of CHK+TIE points (mm)			at CHK points (mm)		
41	87	0	81	10	0	**0.27/0.10**	**0.048**	**0.084**	**0.041**	N.A.	N.A.	N.A.
42	44	43	81	10	0	**0.27/0.10**	**0.047**	**0.082**	**0.040**	0.076	0.125	0.058
43	10	77	81	10	0	**0.26/0.10**	**0.049**	**0.084**	**0.043**	0.097	0.144	0.134
44	168	--	free	10	0	**0.25/0.09**	**0.043**	**0.074**	**0.037**	N.A.	N.A.	N.A.

Table 5. Absolute accuracy test of F828.

Ver	Compression	APs	Rej	Sigma0	STD-X	STD-Y	STD-Z	RMSE-X	RMSE-Y	RMSE-Z
				μm/pixel	of CHK+TIE points (mm)			at CHK points (mm)		
51	1.0 (TIFF - 22.9MB)	10	0	0.26/0.10	0.047	0.082	0.040	0.077	0.120	0.059
52	5.5 (Q100 - 4,2MB)	10	0	0.26/0.10	0.047	0.082	0.040	0.078	0.124	0.059
53	41.6 (Q70 - 0.5MB)	10	0	0.26/0.10	0.047	0.082	0.040	0.077	0.132	0.060

Table 6. JPEG compression test with F828 (GCP/CHK/TIE are 44/43/81 respectively).

Ver	GCP	CHK	TIE	APs	Rej	Sigma0	STD-X	STD-Y	STD-Z	RMSE-X	RMSE-Y	RMSE-Z
						μm/pixel	of CHK+TIE points (mm)			at CHK points (mm)		
61	87	0	99	10	0	0.54/0.25	0.151	0.241	0.130	N.A.	N.A.	N.A.
62	44	43	99	10	0	0.52/0.24	0.147	0.234	0.127	0.381	0.471	0.203
63	10	77	99	10	0	0.49/0.22	0.155	0.245	0.136	0.574	0.636	0.222
64	186	--	free	10	0	0.48/0.22	0.138	0.217	0.116	N.A.	N.A.	N.A.

Table 7. Temporal stability test of N93 (image acquisition on 30th September, 2007).

K750i – image: 12 (version 10)
(a)

N93 – image: 10 (version 21)
(c)

W100 – image: 9 (version 31)
(e)

K750i – image: 16 (version 10)
(b)

N93 – image: 13 (version 21)
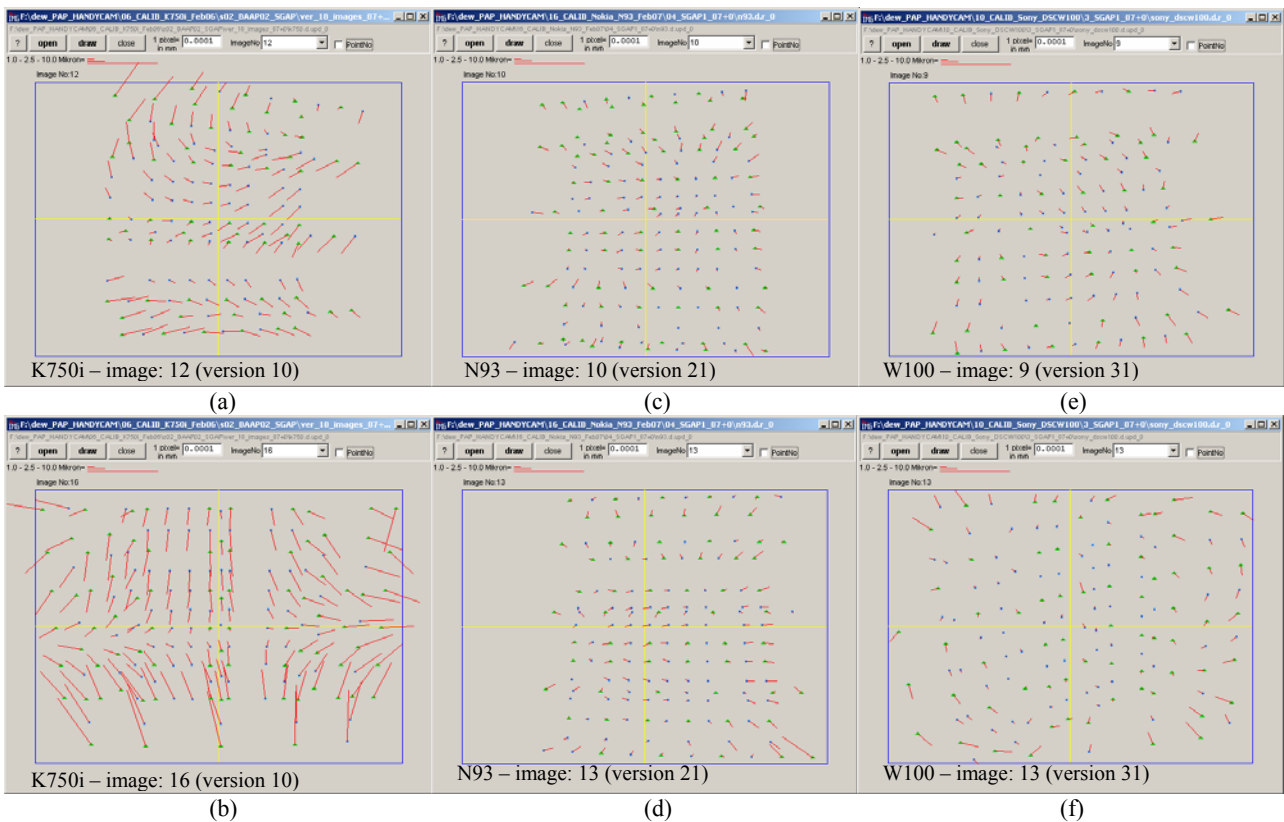(d)

W100 – image: 13 (version 31)
(f)

Figure 7. Systematic residual patterns after the self-calibrating bundle adjustment.

3.5 JPEG test with F828

The use of JPEG images for the image measurements of K750i, N93 and W100 raised the question whether the JPEG compression has an effect on the results. The original TIFF images of the F828 were converted to quality level 100 (maximum quality) and 70 JPEG images, using the free software IrfanView (version 3.98, http://www.irfanview.com/). Table 6 gives the results. The loss of empirical accuracy due to ~ 42 times JPEG compression is only 12 microns in depth (version 51 and 53 in Table 6). The other coordinates are of the same accuracy. Our results are controversial to those results given in Lam et al. (2001), Li et al. (2002) and Shih and Liu (2005). However, their tests are on aerial images, while we have a close-range test object under good illumination conditions.

3.6 Stability test with N93

In order to check the temporal stability of the interior orientation over time, we acquired two sets of images of N93, the first dataset on 6th Februray, 2007 (whose results are given in Chapter 3.2 and in Table 3) and the second on 30th September, 2007. Both datasets have the same number of images and roughly the same acquisition geometry. The numerical results of the second epoch are given in Table 7. The September 2007 dataset has slightly better theoretical precision and empirical accuracy numbers than the February 2007 results. This is because of slightly better convergent image acquisition geometry of September 2007 dataset. We have found similar systematic error patterns also on the September 2007 images (Figure 8a and 8b).

We compared the tie point coordinates of the Version 21 (February 2007) and Version 61 (September 2007) results. The means of the differences (February'07 – September'07) are +0.043, +0.002 and +0.004 mm for the X, Y and Z axes, respectively. The standard deviations of the coordinate differences (0.089, 0.169 and 0.106 mm for X, Y and Z axes, respectively) are considerably smaller than the empirical accuracy numbers.
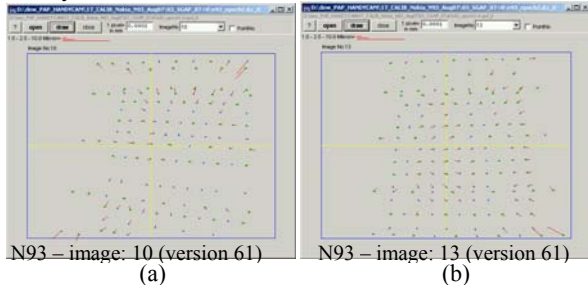

N93 – image: 10 (version 61)   N93 – image: 13 (version 61)
(a)   (b)

Figure 8. Systematic residual patterns of images 10 (a) and 13 (b) of version 61 after the self-calibrating bundle adjustment.

The change of the principal point locations (x_0 and y_0) and the focal length (c) between Version 21 (of February 2007) and Version 61 (of September 2007) are only -1.2, +1.0 and -1.8 microns, respectively. The corresponding standard deviations of the differences (calculated according to the law of error propagation without considering the correlations) are ±1.1, ±0.8 and ±0.6 microns, respectively.

3.7 Image residual analysis

In an image residual analysis we average the directions and the magnitudes of the residual vectors at pre-defined grid locations (in our case at 24 x 18 locations). This shows the nature of the systematic errors remaining after the self-calibrating bundle adjustment (Figure 9). The systematic error pattern of the twelve image version (Figure 9b) of the K50i is similar to the eighteen image version (Figure 9a). We also note that the image residual analysis results of the two epochs' calibration results of the N93 are almost identical (Figure 9c and 9d). The F828 has

the best results with respect to randomness and magnitude of the averaged residual vectors (Figure 9f).

4. ANALYSIS OF RESULTS

In spite of giving the worst results in the test, the K750i still can offer sub-millimeters accuracy in object space. Both block-invariant 10 and 44 additional parameter sets cannot compensate the systematic errors fully.

The cameras K750i, N93 and W100 give identical standard deviation values for the image observations (between 1/4 - 1/5 pixel). They all apply a chip level image enhancement for sharpening the images. This effect is visible in Figures 5a, 5b and 5c. This low level image enhancement, while improving the visual quality, is probably reducing the geometric quality of the cameras. They show noticeably block-variant systematic errors after the self-calibrating bundle adjustment with block-invariant additional parameters.

The N93 and W100 have the same lens systems (Zeiss, Vario-Tessar). The W100 has a CCD sensor of larger size with 8 Mpixels. It is 2.5 times larger than the CMOS sensor of N93. According to theoretical expectations, the N93 should give an accuracy of factor 1.6 (square root of 2.5) worse compared to the W100. The N93 almost strictly meets this expectation by giving 1.7-1.9 times worse numbers than the W100. On the other hand, there is a large difference between those two cameras, considering the size of the imaging system and the cost of the materials used in the construction. In this respect, the accuracy performance of the N93, as compared to the W100, is noteworthy. Although the W100 and F828 have the same image format with 8 Mpixels, the expectation of equal accuracy does not hold here. The W100 gives substantially worse accuracy numbers (almost 3 times) than the F828. This is mainly due to a better lens system of the F828 and (possibly) the degrading chip level image enhancement operation of the W100.
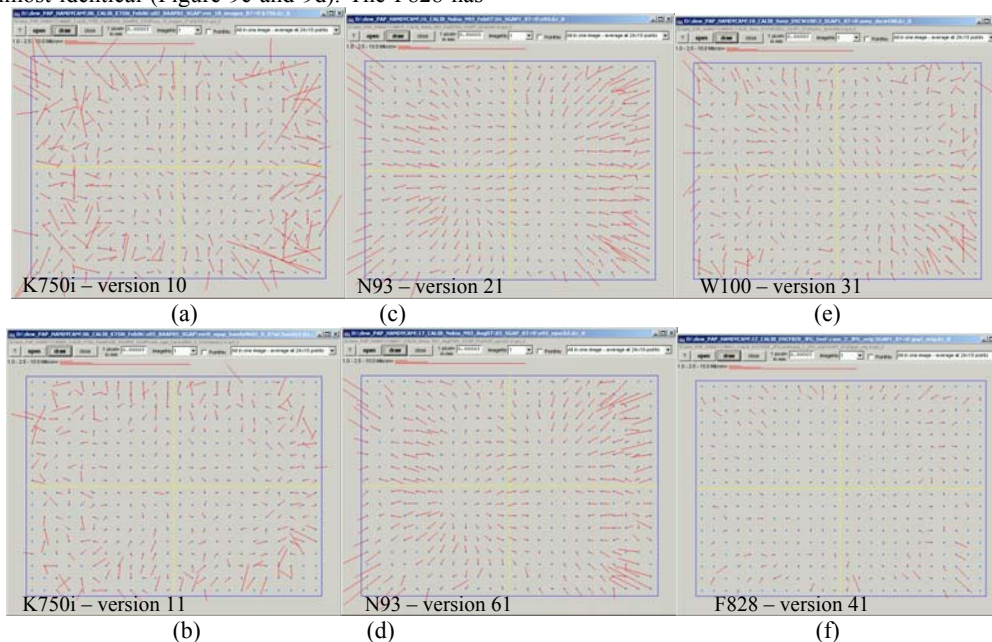

K750i – version 10   N93 – version 21   W100 – version 31
(a)   (c)   (e)

K750i – version 11   N93 – version 61   F828 – version 41
(b)   (d)   (f)

Figure 9. Graphical results of the image residual analysis, based on residual averaging over all images of a particular test configuration.

5. CONCLUSIONS

We have metrically calibrated and we have tested the metric accuracy of four consumer-grade imaging devices: Two mobile phone cameras (Sony Ericsson K750i and Nokia N93) and two still video cameras (Sony DSC W100 and Sony DSC F828). The tests were performed by using our in-house 3D testfield. We have found unwanted effects from image enhancement (sharpening) in the K750i, N93 and W100 cameras and JPEG compression artifacts in the N93. In all four cases we have used (more or less) the same imaging geometry, and imaging conditions in order to make the results comparable. With the given strong geometrical set-up of course all parameters for the interior orientation could be calibrated reliably. The accuracy tests showed that in all cases the theoretical expectations, as defined by the average standard deviations of the object space coordinates, could not be achieved by the empirical RMSEs, computed from checkpoints. The deviations range from factor 3.3 (K750i) to factor 1.7 (F828). While the sigma0 values of the K750i, N93 and W100 are all at a 1/5 pixel level, they drop down to 1/10 pixel with the F828. This improvement in sigma0 is matched by the better behaviour of the post-adjustment image residuals. Only in case of the F828 do we get an almost random distribution. The other cameras, in particular the K750i, suffer from strong image-variant systematic errors. Since we have used in our self-calibration only block-invariant additional parameters these errors could not be compensated. The error patterns are also not in agreement with what we are used to in photogrammetry. Therefore, our standard additional parameter functions cannot compensate these defects. So far we cannot explain the reasons for these errors. Could they lie in the image enhancement procedure or any other shortcomings in the electronic circuits? Nevertheless, and despite these problems, we could reach relative accuracies of 1:8 000 in-plane and 0.03% of average depth with the K750i and 1:34 000 in-plane and 0.005% of average depth with the F828, using in both cases 10 control points. This superior behaviour of the F828 can only partly be explained by the larger image format (8 Mpixels versus 2 Mpixels), which theoretically should only lead to an improvement of factor 2.

If we apply to both cameras a free network adjustment by minimizing the trace of the covariance matrix for the object space coordinates we get the following values: 1:25 000 and 0.009% for the K750i and 1:99 000 and 0.0025% for the F828. This shows roughly the same relationship between both cameras, it gives however a better indication of the potential system accuracy. It is worthwhile to note that, compared to the film-based large format aerial photogrammetric block adjustment accuracy, we can achieve here the same and better accuracies in height and almost the same in planimetry, if we consider for the aerial case an object area of one image coverage only (like in our close-range case). This definitely indicates the great potential of consumer-grade and even mobile phone cameras for photogrammetric processing. The main remaining problem is to find a convincing explanation for the image-to-image varying systematic error pattern in some of the mobile phone cameras.

In a final test we also checked the effect of JPEG compression on the metric system accuracy for the F828 camera. Even when going up to a factor of 42 compression rate we did get only a small reduction in accuracy (9% in depth direction). This can be considered harmless. We spread the tests of the N93 over a longer time period in order to check the temporal stability of the calibration. We observed that the interior orientation of N93 did

not change significantly according to our one dimensional statistical test procedure. We plan to repeat the significance test with a multi-dimensional test.

Our future plan is also to invest some more work into image quality studies. We believe that with a proper calibration and data processing software performance these devices can be used for many photogrammetric tasks which require an accuracy of around 1:10 000. The integration of GPS receivers and motion sensors will further broaden their applicability. Also, it is to be expected that the quality and performance of the integrated cameras will further improve, together with the on-board processing functions. This may allow one day such a device to be used as a stand-alone photogrammetric data acquisition and processing tool, at least for smaller projects. In conclusion we can state that mobile cameras do give us a very interesting option for doing "mobile photogrammetry", in terms of accuracy, costs and flexibility.

REFERENCES

Al-Baker, O., Benlamri, R. & Al-Qayedi, A., 2005. A GPRS-based remote human face identification system for handheld devices. WOCN'05, Dubai, March 6-8, pp. 367-371.

Beyer, H., 1992.Geometric and radiometric analysis of a CCD-camera based photogrammetric close-range system. PhD thesis, IGP, ETH Zurich, Mitteilungen Nr. 51.

Chowdhury, A., Darveaux, R., et al., 2005.Challenges of megapixel camera module assembly and test. Electronic Components and Technology Conference, Spa Lake Buena Vista, Florida, May 31 – June 3, pp. 1390 -1401.

Chung, Y., Jang, D., et al., 2004. Distortion correction for better character recognition of camera based document images. Photonics Applications in Astronomy, Biomedicine, Imaging, Materials Processing, & Education, SPIE Vol.5578, pp. 389-399.

Clemens, G., Sanahuja, F. & Beaugeant, C., 2005. Audio-enhanced panoramic image capturing and rendering on mobile devices. Multimedia and Expo (ICME'05), Amsterdam, July 6-8, pp. 988-991.

Gruen, A., 1978. Progress in photogrammetric point determination by compensating of systematic errors and detecting of gross errors. ISPRS Commission III Symposium, Moscow, pp. 113-140.

Gruen, A., 1985. Adaptive least squares correlation: A powerful image matching technique. *S. Afr. J. of Photogrammetry, Remote Sensing and Cartography*, 14 (3), 175-187

Koga, M., Mine, R., et al., 2005. Camera-based Kanji OCR for mobile-phones: Practical issues. Document Analysis and Recognition, Seoul, August 29 - September 1, pp. 635-639.

Lam, K.W.K., Li, Z. & Yuan, X., 2001. Effetcs of JPEG compression on the accuracy of Digital Terrain Models automatically derived from digital aerial images. *The Photogrammetric Record*, 17 (98), 331-342.

Lenz, R.K. & Tsai, R.Y., 1988. Techniques for calibration of the scale factor and image center for high accuracy 3-D machine vision metrology. IEEE Transactions on PAMI, 10 (5), 713-720.

Li, Z., Yuan, X. & Lam, K.W.K., 2002. Effects of JPEG compression on the accuracy of photogrammetric point determination. *Photogrammetric Engineering &d Remote Sensing*, 68 (8), 847-853.

Myung-Jin, C., 2005. Development of compact auto focus actuator for camera phone by applying new electromagnetic configuration. Optomechatronic Actuators and Manipulation, Sappora, December 5, SPIE Vol. 6048, pp. 60480J-1-9.

Parikh, T.S., 2005. Using mobile phones for secure, distributed document processing in the developing world. *Pervasive Computing*, April-June 2005, 74-81.

Physorg, 2004. Sharp Develops 2-Megapixel CCD Camera Module for Mobile Phones with New 2X Optical Inner Zoom Lens. http://www.physorg.com/news1207.html (accessed on 30.04.07).

Physorg, 2005. Sharp Develops Two New 3-Megapixel CCD Camera Modules for Mobile Phones. http://www.physorg.com/news6096.html (accessed on 30.04.07).

Pittore, M., Cappello, M., Ancona, M. & Scagliola, N., 2005. Role of image recognition in defining the user's focus of attention in 3G phone applications: The AGAMEMNON experience. *Image Processing, Genova*, Italy, Sep. 11-14, pp. 1012-1015.

Riegel, T.B., 2005. MPEG-4 based 2D facial animation for mobile devices. *Multimedia on Mobile Devices*, SPIE Vol. 5684, pp. 55-62.

Rohs, M., 2004. Real-world interaction with camera phones. Ubiquitous Computing Systems, Tokyo, LNCS 3598, pp. 74-89.

Shih, T.-Y. & Liu, J.-K., 2005. Effects of JPEG 2000 compression on automated DSM extraction: evidence from aerial photographs. *Photogrammetric Record*, 20 (112): 351-365.

Ueda, N., Nakanishi, Y., Matsukawa, S. & Motoe, M., 2004. Developing a GIS using a mobile phone equipped with a camera and a GPS, and its exhibitions. Distributed Computing Systems Workshop, Hachioji, Tokyo, March 23-24, pp. 414-417.

Watanabe, Y., Sono, K., Yokomizo, K. & Okada, Y., 2003. Translation camera on mobile phone. Multimedia and Expo, Baltimore, Maryland, July 6-9, pp. II-177-180.

Williams, M., 2006. CeBIT: Samsung Shows 10-Megapixel Camera Phone. PCWORLD, 03/2009, http://www.pcworld.com/article/id,125020/article.html (accessed on 30.04.07).